



Design of a Wideband Slot Bow-tie Antenna Excited by a Microstrip to CPW Transition for Applications in the Millimeter Wave Band

A.E Sanchez Colin, P. Febvre

► To cite this version:

A.E Sanchez Colin, P. Febvre. Design of a Wideband Slot Bow-tie Antenna Excited by a Microstrip to CPW Transition for Applications in the Millimeter Wave Band. Progress In Electromagnetics Research Symposium (PIERS 2009), Aug 2009, Moscow, Russia. pp.1421-1425. <hal-04936641>

HAL Id: hal-04936641

<https://hal.science/hal-04936641v1>

Submitted on 8 Feb 2025

HAL is a multi-disciplinary open access archive for the deposit and dissemination of scientific research documents, whether they are published or not. The documents may come from teaching and research institutions in France or abroad, or from public or private research centers.

L'archive ouverte pluridisciplinaire **HAL**, est destinée au dépôt et à la diffusion de documents scientifiques de niveau recherche, publiés ou non, émanant des établissements d'enseignement et de recherche français ou étrangers, des laboratoires publics ou privés.



HAL Authorization

Design of a wideband slot bow-tie antenna excited by a microstrip to CPW transition for applications in the millimeter wave band

A. Colin¹ and P. Febvre²

¹ Instituto de Física de Cantabria (CSIC-UC). Av. Los Castros s/n. 39005 Santander-Spain.

²IMEP-LAHC, UMR 5130 CNRS, Campus Scientifique, University of Savoie, 73376 Le Bourget du Lac, France

Abstract- We present a compact design of a slot bow-tie antenna excited by a microstrip to coplanar waveguide (CPW) transition, operating at the central frequency of 45GHz in the millimeter wave range from 25 to 65 GHz. Simulation results have shown 85% bandwidth with VSWR < 2 for this antenna. Its small size and symmetric geometry facilitate the integration with microstrip circuits and the connection with active or passive elements. A comparison between normal and superconductive metallization in this design is also presented. This antenna can be used in array configurations for applications in wireless communications, or for astrophysical experiments based on the study of the Cosmic Microwave Background (CMB).

1. INTRODUCTION

Nowadays, studies of the Cosmic Microwave Background (CMB) require observational measurements at different frequency bands; for instance, the anomalous microwave emission is being studied as additional component of the diffuse galactic foregrounds. Previous studies have demonstrated some emission in the frequency range from 11 to 17 GHz [1]. That has also been recently measured at frequencies of ~31 GHz [2] although it can be observed up to 60 GHz but at lower emissivity levels. Some experiments for the CMB detection utilize conical horn antennas to receive the signal and are exposed to the environment temperature whereas the detectors system is cooled inside a cryostat at low temperature, thus giving a wide range of difficulties during the coupling of the setup. Planar array antennas could be useful to avoid some of these difficulties by selecting the correct design and materials, but that implies big challenges in the developments of new detection systems.

Bow-tie slot antennas are widely investigated for many applications where low profile, weigh, size, cost, and ease of installation are required. The bow-tie slot antennas usually present a wider bandwidth in comparison with the narrow bandwidths of the microstrip patch antennas, and have the advantage of a good impedance match and bi-directional radiation patterns. Commonly they are integrated in array systems operating in different bands, sometimes the setup is designed to use separate antennas for each band. With the emergence of new technologies, currently it turns to be possible and desirable to design a single antenna that operates in several bands as broad as possible for a same setup system. The characteristic input impedance of the feed line is one of the deciding factors which is directly associated to the antenna's bandwidth, therefore it must be carefully considered during its design. In this study the length and width of the transition stripline have been crucial for the final design, as well as the choice of the materials. The use of normal metal conductors will lead to increase losses caused by the skin depth of the order of magnitude of the film thickness. To avoid this issue, and since these arrays need to be cooled with the detectors, it is advisable to use superconducting materials.

In this paper we present the computed radiation characteristics for a single element bow-tie slot antenna printed on a commercial alumina substrate plated with gold (*Au*), which is excited by a microstrip to CPW

transition. The feed lines have been computed and optimized using the commercial TXLINE-AWR package in order to keep the good microwave matching properties to the antenna. Then this antenna is compared with two identical antenna-geometries plated with niobium (*Nb*) at its corresponding normal and superconducting states. The antenna's performances were studied in both the unidirectional and bidirectional cases. To achieve the first one, we introduced a metallic reflector plane placed $\lambda_0/4$ below the substrate. All simulations were made under the environment of the HFSS-Ansoft software, which is based on the finite element method.

2. ANTENNA DESIGN

The antenna was designed as bow-tie slot centered on a rectangle ($25.4 \times 28 \text{ mm}^2$) alumina substrate of 0.254 mm thickness with $3\mu\text{m}$ electroplated gold, relative permittivity of 10, and loss tangent of 0.001. The geometry and parameters of the antenna are shown in Fig. 1a), where $a = 0.05$, $b = 0.1$, $c = 0.25$, $d = 7.5$, $e = 0.5$, $f = 10$, $g = 5.65$, $h = 0.1$, and $i = 7.3$. All dimensions are in mm. The bottom ground plane only covers the microstrip lines section (d and e dimensions). The widths of the microstrip line and gaps of the CPW were calculated to provide a characteristic impedance of approximately 50 Ohms, whose transition between them is made by means of a smaller and thinner stripline ($b \times e$ dimensions) of about 73 Ohms. Fig. 1b) shows the experimental setup with a single element that can be attached to a metal mount with silver conductive epoxy (Epo-Tec H20E). The mount represents a metallic structure made of brass material in which a 50-Ohm hermetic seals with a coaxial jack/plug connector (Southwest Microwave, Inc.) could be integrated on its backside. A removable reflector plane is placed below the substrate in order to vary vertically its height. The centered pin-hole permits the connection between the pin-connector and the microstrip. The mount is designed to be used in direct contact with metal surfaces, as well as with the cold plate of cryostats when a low temperature experiment is required.

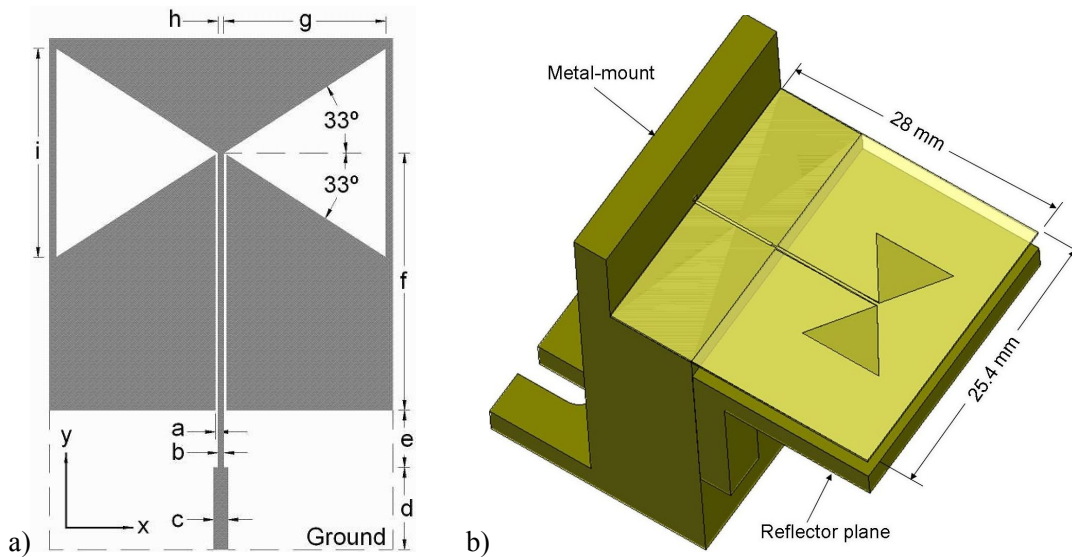


Fig. 1. a) Antenna geometry (not to scale) and parameters: $a = 0.05$, $b = 0.1$, $c = 0.25$, $d = 7.5$, $e = 0.5$, $f = 10$, $g = 5.65$, $h = 0.1$, and $i = 7.3$ (all in mm). Alumina substrate: 0.254 mm thickness, $3\mu\text{m}$ electroplated gold, $\epsilon_r = 10$, and $\delta = 0.001$. b) Experimental setup (not to scale) with a removable reflector plane.

3. SIMULATED RESULTS

For our convenience, all numerical analysis were computed at the frequency $f_0 = 40$ GHz and the reflector plane placed at a distance of $\lambda_0/4$ below the substrate. In all cases we used an excitation wave port of 50 Ohms.

The computed return losses at the bidirectional and unidirectional cases for a single element bow-tie slot antenna metalized with *Au* are shown in Fig. 2 (left). According to these plots, the results show good agreement to each other and present various resonant frequencies over the entire range from 26 to 64 GHz providing around 85% bandwidth. During the design process we noticed the influence of various parameters on the antenna performance. For instance, when one of the dimensions of the transition-stripline is varied, a significant reduction of the total bandwidth and decrease of the input power transmission down to -5 dB have been observed. Fig.2 (right), shows a comparison of the computed return losses for two identical geometries but metalized with *Nb*, more details will be given in section 4.

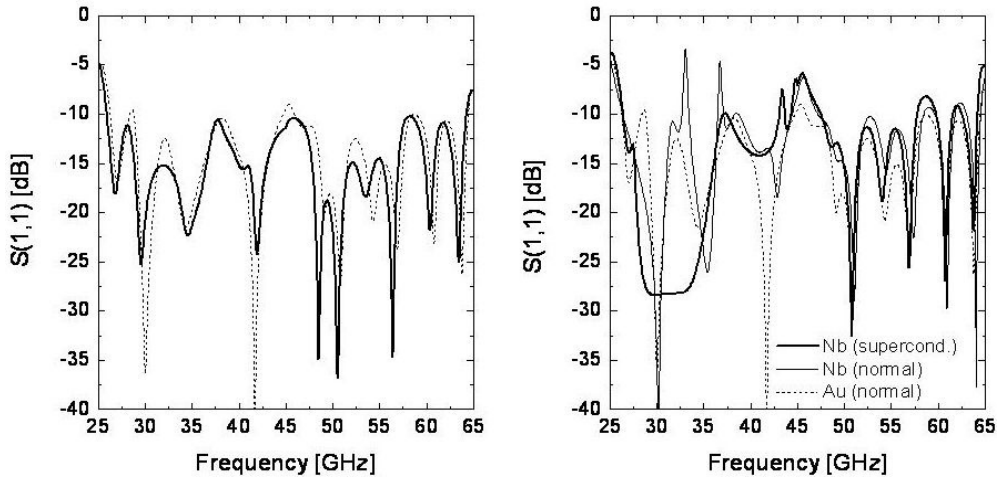


Fig.2. Left: Simulated return losses versus frequency with (dashed line) and without (solid line) reflector plane. Right: Comparison of the return losses between normal and superconducting states of *Nb*.

The computed directivity radiation patterns in the x - z (**H-Plane**) and the y - z (**E-Plane**) at 40 GHz are shown in Fig. 3 (left). The patterns are normalized to a maximum and minimum of 0 and -40 dB respectively, with 10dB/div. The antenna presents an average of -10 dB of cross polarization level and relatively high directivity with a narrow main lobe of around 20° in a beamwidth of 60° for both the E- and H- planes. In wireless communications one antenna can receive the signal from any direction with any polarization; hence this antenna could be utilized for this application. Whereas for the direct detection of specific electromagnetic signals, the antennas must be unidirectional and highly directives; to achieve this, the use of arrays can further improve the radiation patterns increasing the directivity level, as is shown in Fig. 3 (right), in which we simulated a configuration of four elements aligned in the x -direction separated by a distance of $5\lambda_0/3$ (12.5 mm) since it is the optimal free-space distance due to the antenna's geometry. For this case, the directivity level increases by a factor of about 2, thus providing side lobes at -20 dB approximately. In most cases the side lobes can be eliminated using low-pass optical filters for the desired frequency and spherical lenses to focus the entire signal to the receiving antenna which in turn could be connected and coupled to a detector. Therefore this antenna also provides a possibility to be used as an example, in astrophysical studies based in the CMB detection.

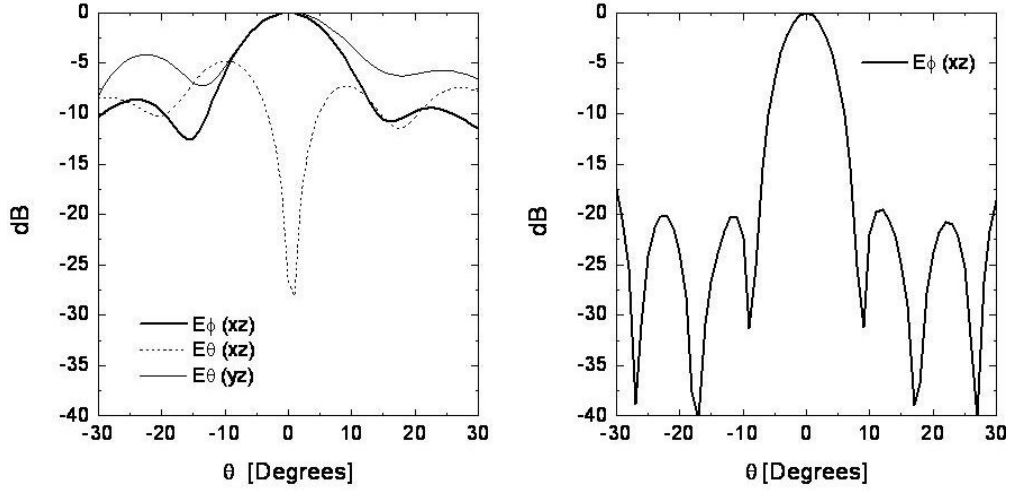


Fig.3. Simulated directivity radiation patterns using a reflector plane for a single element (left), and for a 4-element array separated by $5\lambda_0/3$ (12.5 mm) and aligned in the x -direction (right).

4. COMPARISON BETWEEN NORMAL AND SUPERCONDUCTING METALLIZATION

In order to know the superconducting behavior of this type of antenna, we simulated the full structure by replacing the Au by normal and superconductive Nb , but conserving the geometry and all the parameter dimensions. The simulations were made in two runs: the first one considers the metallization as normal metal but take into account the surface resistance in both electrodes, whereas the second one replaces the superconductive material by boundary surfaces with purely reactive surface impedance (a complete description for understanding this strategy is described in [3-4], in which is taken into account the kinetic inductance inherent to the superconducting state of Nb at 0.1 K). Although it is unusual to utilize thick films with superconductors, in these simulations we utilized them but only for comparative purposes. As we have seen in Fig. 2 (right), the comparison of the return losses show a very good matching for superconductive Nb but only in the frequency range from 26 to 43 GHz since the entire frequency band is divided into two parts. In contrast the normal state of Nb does not present good matching in the first part but in the second one, however we observed a very narrow bandwidth with a prominent resonant frequency centered around 30 GHz with a good matching.

The theoretical analysis was made following the methodology established in [4], and applied separately only to each section of the transmission feed line, as the microstrip line (MSL), the microstrip transition (MST) and the coplanar waveguide (CPW). In all cases we considered the London penetration depth as $\lambda_L = 85$ nm for bulk Nb . For convenience, we present only three of those equations given in [4] for the characteristic impedance (Z_0).

$$Z_{Wheeler}(w', h, \epsilon_r) = 30 \sqrt{\frac{2}{\epsilon_r + 1}} \ln \left\{ 1 + \left(\frac{4h}{w} \right) \left[\left(\frac{14 + \frac{8}{\epsilon_r}}{11} \right) \left(\frac{4h}{w} \right) + \sqrt{\left(\frac{14 + \frac{8}{\epsilon_r}}{11} \right)^2 \left(\frac{4h}{w} \right)^2 + \frac{1 + \frac{1}{\epsilon_r}}{2} \pi^2} \right] \right\} \quad (1)$$

$$Z_0 = Z_{vacuum} \sqrt{\frac{\mu_{eff}}{\epsilon_{eff}}} \frac{h}{w_{eff}} \quad (2)$$

$$Z_0^t = Z_{\text{vacuum}} \sqrt{\frac{\mu_{\text{eff}}}{\epsilon_{\text{eff}}^t}} \frac{1}{4g_1} \quad (3)$$

Eq. (1), proposed in [5], was used to compute Z_0 as normal metals in the MSL and MST. For superconducting metals in the MSL and MST we used Eq. (2), here the analysis was made considering thin superconducting films of 250 nm thickness, with a silicon (SiO) lossless insulator of 200 nm thickness, and $\epsilon_r = 5.7$. In this part of the analysis we found that by conserving the geometry dimensions of each line, the required Z_0 , is reduced down to very low values associated to the very high aspect ratio of MSL. Finally Eq. (3) could be used in all cases for both the normal and superconducting states in the CPW. A summary of the simulated and computed results are shown in Table 1. Additionally the computed effective permittivity is also indicated.

Table 1. Comparison between analytical and 3D modeling results.

	Normal (Au) Thick film				Normal (Nb) Thick film				Superconducting (Nb) Thin film			
	TXLINE		HFSS		EQ. (1)&(3)		HFSS		EQ. (2)&(3)		HFSS	
	Z_0	ϵ_{eff}	Z_0	ϵ_{eff}	Z_0	ϵ_{eff}	Z_0	ϵ_{eff}	Z_0	ϵ_{eff}	Z_0	ϵ_{eff}
MSL	50.67	7.31	42.26	7.43	49.35	6.66	42.01	7.47	0.172	5.69	0.167	5.59
MST	73.24	6.71	63.27	6.83	72.11	6.31	63.49	6.82	0.425	5.51	0.38	5.22
CPW	51.10	5.16	50.18	5.30	49.70	5.06	50.89	5.36	0.169	4.28	0.153	2.81

5. CONCLUSIONS

Simulated and analytical results for bow-tie slot antennas plated with normal and superconducting metals have revealed feasibility and good expectation to be confirmed with the measurements of our prototypes.

Comparison between analytical formulas and HFSS simulations show a good agreement for superconducting structures which is promising to replace time-consuming simulations with simpler formulas whenever possible for the typical geometries.

REFERENCES

1. Watson, R.A. et al, "Detection of anomalous microwave emission in the Perseus molecular cloud with the COSMOSOMAS experiment", *ApJ*, 624:L89, 2005.
2. Dickinson C. "Anomalous emission from HII regions", *CMB Component Separation and the Physics of Foregrounds*, Pasadena California, USA, 14-18 July 2008.
3. Raully D. A. Monfardini, A. Colin, and P. Febvre. "Design of two-band 150-220 GHz superconducting bolometric detection structure," *PIERS Proceedings, Cambridge, USA, July 2-6, 2008*, 852-856.
4. Febvre ,P., C. Boutez, S. George and G. Beaudin, "Models of superconducting microstrip and coplanar elements for submillimeter applications," *Proc. of the Int. Conf. on Millimeter and Submillimeter Waves and Applications II*, vol. SPIE 2558, pp. 136-147, San Diego Convention Center, 9-14 July 1995.
5. Wheeler H.A., "Transmission-Line Properties of a Strip on a Dielectric Sheet on a Plane," *IEEE Trans. Microwave Theory Tech.*, vol. MTT-25, pp. 631-647, Aug. 1977.